Article:
Gheisari, R., Chamberlain, H., Chi-Tangyie, G. et al. (2020) Multi-material additive manufacturing of low sintering temperature Bi2Mo2O9 ceramics with Ag floating electrodes by selective laser burnout. Virtual and Physical Prototyping, 15 (2). pp. 133-147. ISSN: 1745-2759

https://doi.org/10.1080/17452759.2019.1708026

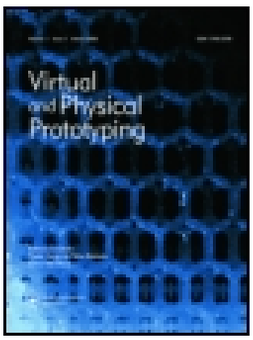

Virtual and Physical Prototyping

ISSN: 1745-2759 (Print) 1745-2767 (Online) Journal homepage: https://www.tandfonline.com/loi/nvpp20

Multi-material additive manufacturing of low sintering temperature $Bi_2Mo_2O_9$ ceramics with Ag floating electrodes by selective laser burnout

Reza Gheisari, Henry Chamberlain, George Chi-Tangyie, Shiyu Zhang, Athanasios Goulas, Chih-Kuo Lee, Tom Whittaker, Dawei Wang, Annapoorani Ketharam, Avishek Ghosh, Bala Vaidhyanathan, Will Whittow, Darren Cadman, Yiannis C. Vardaxoglou, Ian M. Reaney & Daniel S. Engstrøm

To cite this article: Reza Gheisari, Henry Chamberlain, George Chi-Tangyie, Shiyu Zhang, Athanasios Goulas, Chih-Kuo Lee, Tom Whittaker, Dawei Wang, Annapoorani Ketharam, Avishek Ghosh, Bala Vaidhyanathan, Will Whittow, Darren Cadman, Yiannis C. Vardaxoglou, Ian M. Reaney & Daniel S. Engstrøm (2020): Multi-material additive manufacturing of low sintering temperature $Bi_2Mo_2O_9$ ceramics with Ag floating electrodes by selective laser burnout, Virtual and Physical Prototyping, DOI: 10.1080/17452759.2019.1708026

To link to this article: https://doi.org/10.1080/17452759.2019.1708026

Published online: 06 Jan 2020.

VIRTUAL AND PHYSICAL PROTOTYPING
https://doi.org/10.1080/17452759.2019.1708026

Taylor & Francis
Taylor & Francis Group

Multi-material additive manufacturing of low sintering temperature $Bi_2Mo_2O_9$ ceramics with Ag floating electrodes by selective laser burnout

Reza Gheisari [a], Henry Chamberlain[a], George Chi-Tangyie[b], Shiyu Zhang[a], Athanasios Goulas[a], Chih-Kuo Lee[a], Tom Whittaker[a], Dawei Wang[c], Annapoorani Ketharam[b], Avishek Ghosh[b], Bala Vaidhyanathan[b], Will Whittow[a], Darren Cadman[a], Yiannis C. Vardaxoglou[a], Ian M. Reaney[c] and Daniel S. Engstrøm[a]

[a]School of Mechanical, Electrical and Manufacturing Engineering, Loughborough University, Loughborough, UK; [b]Department of Materials, Loughborough University, Loughborough, UK; [c]Department of Materials Science and Engineering, University of Sheffield, Sheffield, UK

ABSTRACT

Additive manufacturing (AM) of co-fired low temperature ceramics offers a unique route for fabrication of novel 3D radio frequency (RF) and microwave communication components, embedded electronics and sensors. This paper describes the first-ever direct 3D printing of low temperature co-fired ceramics/floating electrode 3D structures. Slurry-based AM and selective laser burnout (SLB) were used to fabricate bulk dielectric, $Bi_2Mo_2O_9$ (BMO, sintering temperature = 620–650°C, $\varepsilon_r = 38$) with silver (Ag) internal floating electrodes. A printable BMO slurry was developed and the SLB optimised to improve edge definition and burn out the binder without damaging the ceramic. The SLB increased the green strength needed for shape retention, produced crack-free parts and prevented Ag leaching into the ceramic during co-firing. The green parts were sintered after SLB in a conventional furnace at 645°C for 4 h and achieved 94.5% density, compressive strength of 4097 MPa, a relative permittivity (ε_r) of 33.8 and a loss tangent (tan δ) of 0.0004 (8 GHz) for BMO. The feasibility of using SLB followed by a post-printing sintering step to create BMO/Ag 3D structures was thus demonstrated.

ARTICLE HISTORY
Received 15 September 2019
Accepted 13 December 2019

KEYWORDS
Additive manufacturing; metamaterials; multi-material 3D printing; selective laser burnout; co-fired ceramics

1. Introduction

Additive manufacturing (AM) is a novel technology for producing prototypes as well as functional parts in a layer by layer manner. AM technologies have recently gained increased importance, as they allow production of complex geometries with high levels of accuracy and repeatability in a cost-effective way. A variety of different AM techniques capable of fabricating 3D ceramic parts have been developed over the past years, such as stereolithography, fused deposition of ceramics (FDC), selective laser sintering/melting (SLS/M), and slurry-based 3D printing (Hinczewski, Corbel, and Chartier 1998; Jafari et al. 2000; Chartier et al. 2002; Griffith and Halloran 2005; Liu et al. 2007). Jafari et al. (2000) developed an FDC machine to print green ceramic filaments and successfully made lead zirconate titanate (PZT) components with no observation of defects or delamination. The main disadvantage of FDC is the low resolution and the large amount of polymer in the green body which can require extremely slow burnout process with low densification (Feilden 2017). Yen (2012) developed a new slurry-based sequential layer manufacturing for fabricating ceramic green parts composed of SiO_2 powder using selective laser scanning. The investigated process derived gelling effect from water vaporisation generated by a hot air blower, so a uniform gelled layer without ablation was achieved before building 2D pattern with selective laser scanning and heat treatment in a conventional furnace, subsequently. Tang and Yen (2015) employed the SLB process to produce alumina green parts and replace the sheet material used in the process of laminated object manufacturing (LOM) which was costly, time consuming and required more space. An additional drying step was implemented prior to laser scanning likewise.

The attention of many researchers has now turned to AM of multi-material structures and a variety of AM processes capable of fabricating such structures have recently emerged with improved printing resolution. These techniques are developing rapidly owing to the capability of making composite structures that obtain their unique properties (e.g. mechanical, electrical, etc.) through a single component made of different materials (metal, ceramic, and polymer). Among the leading AM techniques, robocasting is highly utilised technique which takes advantage of computer-controlled robotic

CONTACT Reza Gheisari r.gheisari@lboro.ac.uk School of Mechanical, Electrical and Manufacturing Engineering, Loughborough University, LE11 3TU, UK

system capable of depositing colloidal suspensions to create 3D structures with a wide range of materials and reduced fabrication cost (Tuttle et al. 2001; Lewis et al. 2006; Lu et al. 2009; Cai et al. 2012; Maazouz et al. 2014; Jakus et al. 2015; Zhao et al. 2017; Peng et al. 2018). Since the process is in a layered manner, it is feasible to tailor the properties of such components by controlling the dimensions of its features.

Laser engineered net shaping has been used to produce Ti-6Al-4V with silicon carbide composite coatings to improve its wear resistance (Das et al. 2010). Similar process was used to manufacture compositionally gradient structures of vanadium carbide (VC) and stainless steel 304 (SS304) that exhibited higher hardness and wear resistance (Gualtieri and Bandyopadhyay 2018). Fabrication of Ti-Al_2O_3 compositionally graded structures to evaluate the capability of making a metal-ceramic composite via laser AM has also been successfully demonstrated (Zhang and Bandyopadhyay 2018). Overall, AM of metals and ceramics has been an area of interest as it allows manufacturing of components with outstanding properties compared to conventional alloys (Man et al. 2001; Pang, Man, and Yue 2005; Nurminen, Näkki, and Vuoristo 2009; Balla, Bose, and Bandyopadhyay 2010; Zheng, Chen, and Lian 2010; Das et al. 2011; Zhong et al. 2014; Zhang, Sahasrabudhe, and Bandyopadhyay 2015; Sahasrabudhe and Bandyopadhyay 2016). However, fitting metals and ceramics into one component using AM is still at the early stages of investigation to overcome the current limitations such as sintering/melting temperature mismatch, dimensional accuracy and chemical compatibility of different materials to make functional components for practical systems.

Low temperature co-fired ceramics (LTCC) applications include wireless telecommunication, electronic warfare, satellite broadcasting, and intelligent transport systems (Ziolkowski 2003; Parke et al. 2015; Sebastian, Wang, and Jantunen 2016; Zhang, Whittow, and Vardaxoglou 2017; Wang et al. 2018; Zhou et al. 2019; Faouri et al. 2019). The growth of the mobile phone market in the 1990s led to extensive research and development in temperature stable, medium permittivity dielectric ceramics with applications such as resonators in filters for microwave (MW) communications. Owing to extremely low dielectric loss (high quality factor) and high permittivity, these materials facilitate the fabrication of smaller components with reduced fabrication cost and better performance (Reaney and Iddles 2006). LTCC modules are routinely made by stacking green dielectric layers upon which printed circuitry has been inscribed followed by co-firing to make a dense 3D circuit. Connection between layers are formed via soldering. A significant advantage of the slurry-based 3D printing is that it uses formulations identical to those in conventional tape casting and screen printing and can produce multi-material structures.

LTCC ceramics are known to undergo controlled densification at relative low temperatures with respect to associated internal electrodes. Most LTCC modules require temperature stable low loss (tan $\delta < 0.001$) dielectrics ($10 < \varepsilon_r < 60$) compounds that densify at <900°C and do not react with Ag internal electrodes. BMO has been reported (Sebastian, Wang, and Jantunen 2016; Cho et al. 2005; Zhou et al. 2008, 2009; Zhou et al. 2010) in part to satisfy these criteria with a densification temperature ~645°C, $\varepsilon_r = 38$ and tan δ~0.0002 at MW frequencies but is known to partially react with Ag on co-firing.

Artificial dielectrics and metamaterials have extraordinary properties and can control electromagnetic (EM) wave propagation and tailoring EM properties (Zhang, Whittow, and Vardaxoglou 2017). Currently, manufacturing of metamaterials is costly and time consuming as several processes are required such as micromachining, etching and assembling (Ziolkowski 2003; Parke et al. 2015; Walia et al. 2015). Laser AM of ceramics and metals offers an alternative manufacturing method. To date however, multi-material 3D structures have only been fabricated by heat treating the sample in a furnace layer by layer which causes interfacial reaction by electrode (e.g Ag) migration and stress due to mismatched shrinkage rates and thermal expansion coefficients. The AM technique described in this contribution results in reduced process time, less material waste, lower cost fabrication, and potentially greater material system compatibility for integrated metal/ceramic architectures. The process is the first step towards highly dense ceramics with great geometric design freedom, capable of complex metal/ceramic structures with geometric potentials beyond traditional LTCC, such as 3D metamaterials and metacomponents.

2. Materials and methods

2.1. Slurry preparation

2.1.1. BMO slurry

The $Bi_2Mo_2O_9$ (BMO) powder was synthesised by the solid-state reaction method. Raw chemicals Bi_2O_3 (99.9%, Acros Organics) and MoO_3 (>99%, Acros Organics) were weighted stoichiometrically (Bi_2O_3: MoO_3 = 1:2) and planetary ball-milled in isopropanol for 4 h. Afterwards, the dried mixed powders were calcined for 4 h at 630–650°C (Zhou et al. 2009). Further ball-milling was carried out to reduce the average particle size to 1–5 µm (Figure 1(a)) to minimise nozzle clogging induced by the presence of large particles. The ceramic slurry was prepared by mixing 81 wt.% BMO powder in a ball-mill (Fritsch Pulverisette 7 Micro Mill) with 14 wt% ethylene

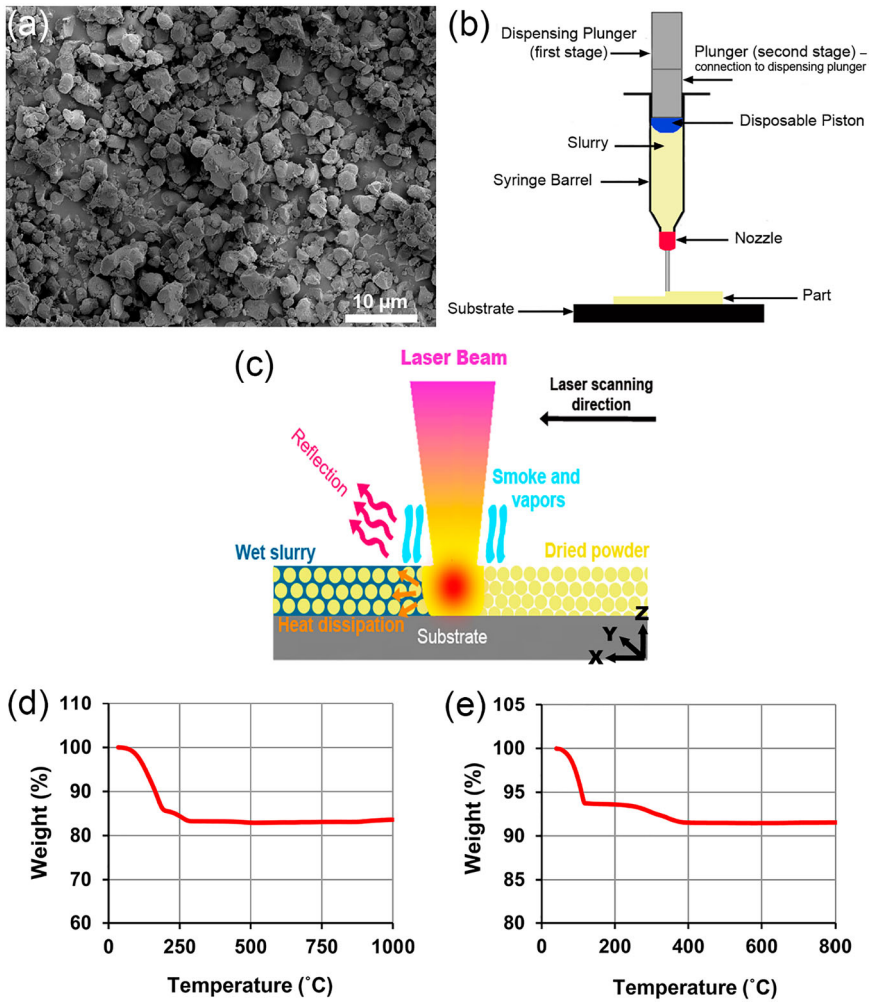

Figure 1. (a) SEM image of BMO powder, (b,c) Illustration of the SLB process; slurry deposition and laser burnout, respectively, (d,e) TGA analysis of the BMO slurry and the Ag paste, respectively.

glycol dimethacrylate, 3 wt.% propylene carbonate and 2 wt% diisononyl phthalate to achieve appropriate viscoelastic properties for 3D printing. It was purposely made with a low viscosity for several reasons:

(1) The slurry flows slightly after deposition filling in gaps between the individual tracks, thereby minimising the porosity.
(2) Pressure drops during printing and air bubbles in the slurry creates discontinuities in the print which is filled in by subsequent layers because of the relatively low viscosity.

2.1.2. Ag paste

The conductive Ag paste (PMC3 silver, Mitsubishi Materials Trading Corporation) was used to print the floating electrodes. It consists of 90 wt.% Ag particles (<5um), an organic binding agent and water. It can be fired at temperatures between 600°C and 900°C and has a low shrinkage (approximately 10%). The silver paste used in this study has been chosen due to its ideal rheological properties that make it a good choice for the proposed AM technique in terms of printability. Through the SLB process and furnace sintering all the additives are burned off and what remains is pure silver unlike the conventional pastes containing glass frit. Conventional Ag pastes with glass frit has also a low storage modulus making only thin structures possible and is therefore not suitable to print in the 3rd dimension. Additionally, the conductivity of the used paste is higher (5.7×10^6 S/m) than the commonly used pastes ($1.75–4.63 \times 10^6$ S/m) and the shrinkage rate of that is very close to the shrinkage rate of the BMO. Thus, the shrinkage rate mismatch is reduced.

2.2. 3D printing

The fabrication process uses layered slurry dispensing followed by selective laser burnout (SLB) to fabricate

mono-material (ceramic only) and multi-material (ceramic/silver) green parts. During the SLB process, binder and solvent are removed from the layers by localized laser heating so that only the inorganic ceramic remains which is lightly sintered, maintaining its rigidity. After sintering the SLB green body densified to ~95% theoretical and its dielectric and mechanical properties measured along with an assessment of its microstructure. Finally, a co-sintered BMO/Ag floating electrode multi-material was 3D printed and sintered following similar procedures to that described below for mono-material parts.

Printing and laser processing experiments were carried out using an OurPlant XTec system (Häcker Automation GmbH, Schwarzhausen, Germany) equipped with a DX-30 syringe dispensing module, using 3 mL syringe barrels and 610 µm diameter tapered tips (Nordson EFD, Aylesbury, United Kingdom) and a Coherent-DILAS InGaAs fiber-coupled multimode diode laser (DILAS Diodenlaser GmbH, Mainz, Germany), operating at a wavelength of 980 ± 10 nm, producing a beam of 330 µm diameter.

The BMO slurry was extruded onto an Al_2O_3 substrate located on the base platform with a controlled flowrate (0.3 µl/s) through a circular nozzle ($d = 610$ µm), Figure 1(b). Once the deposition of a layer was complete, it was scanned with a low laser energy density so that generated heat is conducted into the wet layer to uniformly burn out the organic components of the slurry with only ceramic powder remaining without sintering/melting that, Figure 1(c).

It is worth-mentioning that mechanism of heat distribution and dissipation is identical to that in the SLS process (Sofia, Barletta, and Poletto 2018). However, during the SLS process high energy densities are applied to consolidate powder particles and achieve full densification. During the SLB, laser beam is irradiated and generates a hot spot on the deposited layer. Thus, the top surface of the layer is heated up first by absorbing incident photons. After the local temperature reaches a stable state (corresponding to the melting point of the binder), the generated heat flows down from the surface to the centre of the layer. Eventually, heat transfer determined by the surrounding powder and binder properties causes heat conduction within the layer with a partial reflection and dissipation of the radiated energy. Laser scanning was carried out in X and Y directions for each layer. The vector spacing (V_S) in X and Y direction was set to 200 µm.

When laser scanning of a layer was complete, the dispensing head was offset by 100 µm in the Z direction which defined the height of the next layer to be deposited. Eventually, the fabricated samples were sintered in a conventional furnace at 645°C for 2–5 h to obtain a dense and homogeneous body with a stable thickness for further characterisation.

Thermal gravimetric analysis (TGA), as shown in Figure 1(d,e), was performed on the slurries to determine the binder burnout temperature. The BMO slurry showed a 19% decrease in mass between 70°C and 260°C while the Ag paste showed 8.5% weight loss between 50°C and 390°C which corresponds to binder burn out with no further mass lost up to 1000°C.

To determine the appropriate conditions for SLB with respect to the BMO slurry, four laser power increments were tested; 1.5, 2.5, 3.5 and 4.5 W and four scanning speeds; 10, 20, 30, 40 mm/sec, giving energy densities (Tian et al. 2009) from 0.18 to 2.25 J/mm^2. The weight of each sample after the slurry had been deposited was compared to that after laser processing to calculate the mass of material removed. The laser was passed over the sample multiple times until the weight stabilised.

2.3. Characterisation

Micrographs were collected using a JEOL 7800F scanning electron microscopy (SEM). Powders samples were characterised using the same SEM device and a Malvern Mastersizer 2000 laser diffraction based particle size analyser. The phase assemblage of sintered bodies identified using Bruker D2 PHASER X-ray diffractometer. TGA analysis for the dried slurry was carried out with a TA Instruments Q5000 IR. Compression test was performed using a an Instron 3369 for samples of 10 mm × 10 mm × 3 mm. In addition to density measurements which was performed using Archimedes technique, percentage of porosity was calculated by using ImageJ software that converted images into a binary code. ε_r for the $Bi_2Mo_2O_9$ samples of 22.86 mm in length, 10.16 mm in width and 1.5 mm in height were obtained using Anritsu ShockLine Vector Network Analyzers (MS46522B) between 8 and 12 GHz. BMO pellets were also measured using the $TE_{01\delta}$ dielectric resonator method with a vector network analyser (R3767CH, Advantest Corporation, Tokyo, Japan).

3. Results and discussion

The final weight loss and the number of necessary passes are shown in Figure 2(a) for the tested laser powers and scan speeds. Figure 2(b) shows that the onset of full laser burn out occurs at 0.41 J/ mm^2 (equivalent to 2.5 W laser power and 30 mm/s scan speeds). The theoretical limit for the weight loss is 19% (Figure 1(d)) but this value is exceeded or receded for several samples, possibly due to uneven printing caused by slurry segregation whilst

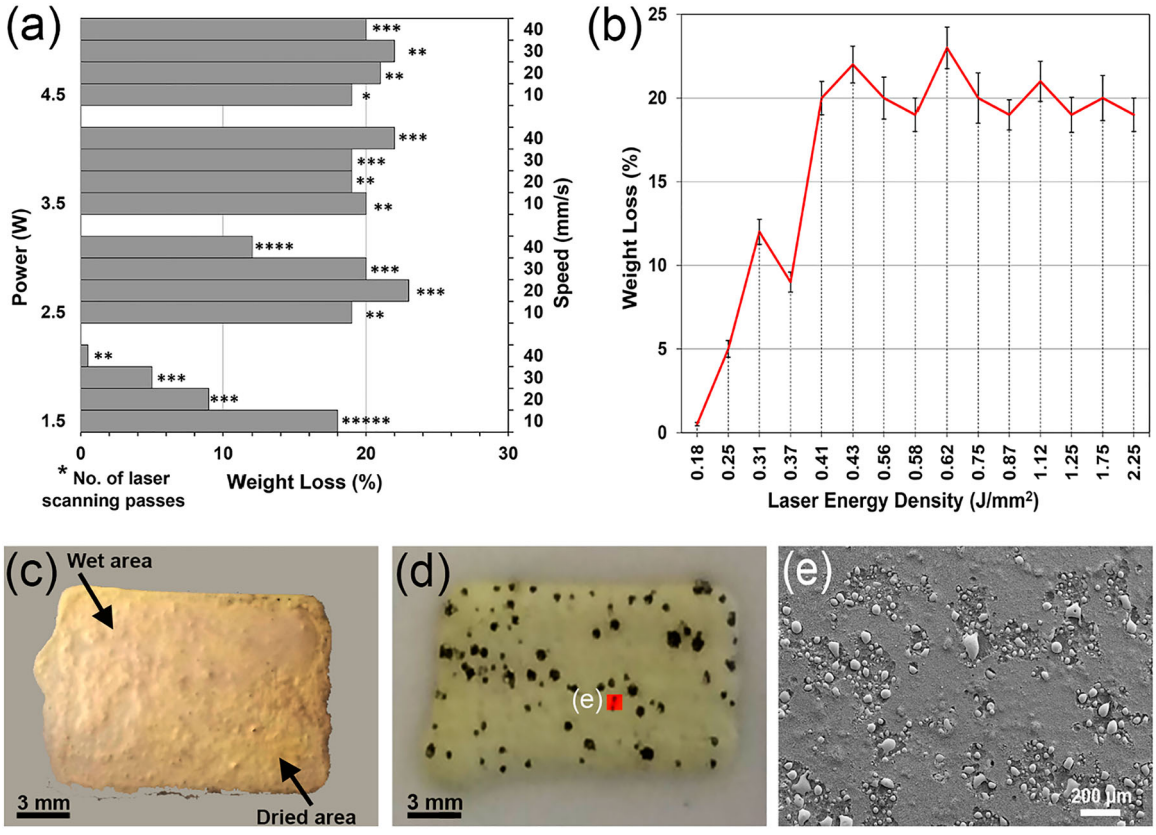

Figure 2. (a,b) Weight loss percentage of the deposited layers after laser burnout process according to the laser power, scanning speed, number of scanning passes and laser energy density (five samples of 10 mm × 10 mm × 100 µm for each set of parameters combinations) with a fixed vector spacing (200 µm), (c) Incomplete binder burnout when the layer was scanned at a low laser energy density, (d,e) local melting ascribed to excessive laser energy density.

in the syringe which results an uneven binder/solvent/ceramic ratio during deposition. The printed green bodies shrank by 15 ± 0.84% in length, 14 ± 0.65% in width, and 3.22 ± 0.18% in height after laser burnout.

At lower energy density, the laser does not fully remove the solvent and binder as shown in Figure 2(c), resulting in spreading of the material rather than binder burn-out. For a laser energy density above 0.41 J/ mm^2, black deposits were observed within the printed layers which currently remain unidentified (Figure 2(d)). This by-product of the process is, however, undesirable and would become embedded in the ceramic upon further deposition. Moreover, higher energy densities induce local heterogeneous melting as shown in Figure 2(d,e) which destroys the printed geometry and creates an inhomogeneous microstructure detrimental to MW properties. In summary, 2.5 W, 30 mm/s, and V_S = 200 µm were chosen as the laser scanning parameters to not only avoid damaging the layers but to also limit the number of passes thereby reducing processing time.

Figure 3(a,b) show BMO green bodies fabricated using the same slurry, design and print parameters without and with SLB, respectively. There is a significant difference between the produced samples in terms of dimensional accuracy and edge definition which further justifies the application of laser scanning. Figure 3(a) demonstrates the poor geometric retention, 13 mm (length) × 7.5 mm (width), due to a combination of capillary action and fluidity of the material when SLB is not employed. In contrast, the SLB process (Figure 3 (b)) results in a fine edge definition and superior dimensional accuracy, 8 mm (length) × 4.5 mm (width). We note that with further optimisation, better edge definition may be possible without SLB but we emphasise that SLB facilitates slurry-based 3D printing with low viscosity slurries for high resolution printing.

During SLB some ceramic particles have ablated onto the substrate by rapid vaporisation of the solvent and additives. This phenomenon can result in increased surface roughness of the green part (Yen 2012). Gases can also be seen around the laser spot during binder burnout due to chemical reactions with the organics and partial ablation of BMO powder. The effect of the laser beam on the microstructure is evident in Figure 3. At low magnification, pits up to 1 mm long in the direction that the laser raster are present on the surface of the

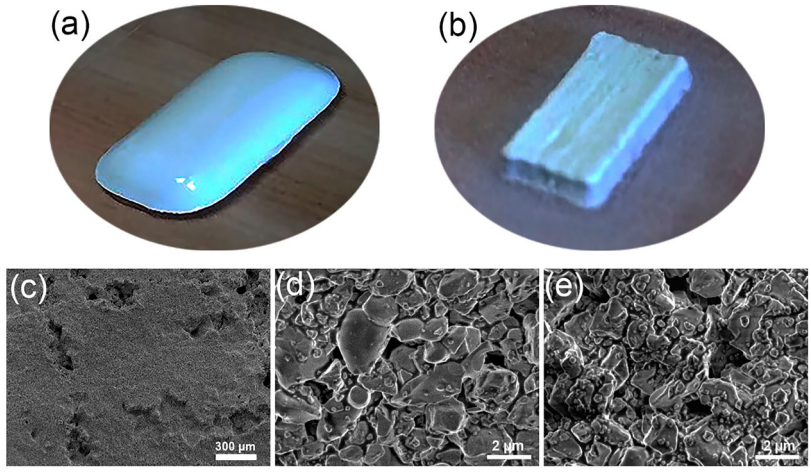

Figure 3. (a,b) Non-laser irradiated and laser irradated green bodies fabricated using same slurry deposition technique, respectively. SEM images of (c) surface damages caused by the laser, (d) microstructure of a non-laser irradiated layer, and (e) microstructure of a laser irradiated layer.

green layers (Figure 3(c)) but are filled by the next layer deposited. At higher magnification (Figure 3(d,e)), non-laser irradiated and laser irradiated layers are similar so that the SLB process causes only minor microstructural effects on the ceramic. As it was mentioned earlier, the raw powder was ball-milled to reduce the average particle size to approximately 5 µm. However, controlling the particle size through ball-milling process is difficult and having small particles (≤1 µm) within the powder distribution is inevitable. Therefore, it can be inferred that when laser irradiates the layer to burnout the binder, these very small particles are lifted to the surface by vaporisation pressure, Figure 3(e).

To find the optimum dwell time, samples were sintered in the furnace at 645°C for 2, 3, 4 and 5 h. Figure 4(a–d) presents the surface morphologies of the sintered $Bi_2Mo_2O_9$ ceramics for the investigated dwell times, respectively. Incomplete sintering occurred when the dwell time was <4 h. Porosity decreased with increasing the dwell time to 5 h with a sharp drop between 3 and 4 h. The ceramic samples sintered for 4 h showed a dense structure (≃94.5 ± 2%) with no evidence of filaments or layer gaps from the print process (Figure 4(e)).

Properties of the SLB/sintered BMO samples are listed in Table 1. Density and porosity significantly affect the mechanical strength of ceramics along with macroscopic defects. The total porosity in the SLB/sintered samples is ~5.5%, potentially caused by laser interaction during binder burnout which increases surface roughness (Figure 3(c)). Although the SLB may not volatilise all the binder, the final sintering step ensures that all the organics are removed.

It is worth-mentioning that particular care must be taken when synthesising and manufacturing ceramic powders to ensure optimum properties. Otherwise, nominal changes can result in different batches of material with variable properties and temperature stability (e.g. shrinkage rate). The comparison of surface microstructures in Figure 4(a–e) reveals the growth of a plate-like phase between grains perpendicular to the surface of the samples. Figure 5 shows the X-ray diffraction spectra from the BMO green body fabricated by SLB and fully sintered BMO sample. All major peaks are indexed as a single monoclinic phase (space group, $P2_1/n$) identical to the raw powder. Although a dense microstructure is achieved, Bi_2MoO_6 and $Bi_2Mo_3O_{12}$ minor secondary phases are present. The plate-like structures in Figure 4(a–d) is most likely Bi_2MoO_6 since this phase has a plate like morphology due to its layered crystal structure (Aurivillius) and the higher secondary XRD intensity is due to increased crystallinity after sintering (Liu et al. 2010).

Figure 6(a) shows a rectangular sample of BMO fabricated by SLB after furnace sintering, but post-SLB sintering also allowed the fabrication of more complex shapes, Figure 6(b,c). The suspended beam was deposited over a 3D printed PVA block that was burnt away during furnace sintering. The use of PVA as pre-prepared support material was particularly effective for the bridge structure. The PVA blocks ensured that shape of the green body was maintained not only during the fabrication process but also until sintering was complete. For more complex suspended shapes, a multi-nozzle printer can be used. A multi-nozzle printer will also be needed for further design freedom in fully dense multi-material structures such as BMO/Ag microwave electronics with a close match in shrinkage and thermal expansion between the materials.

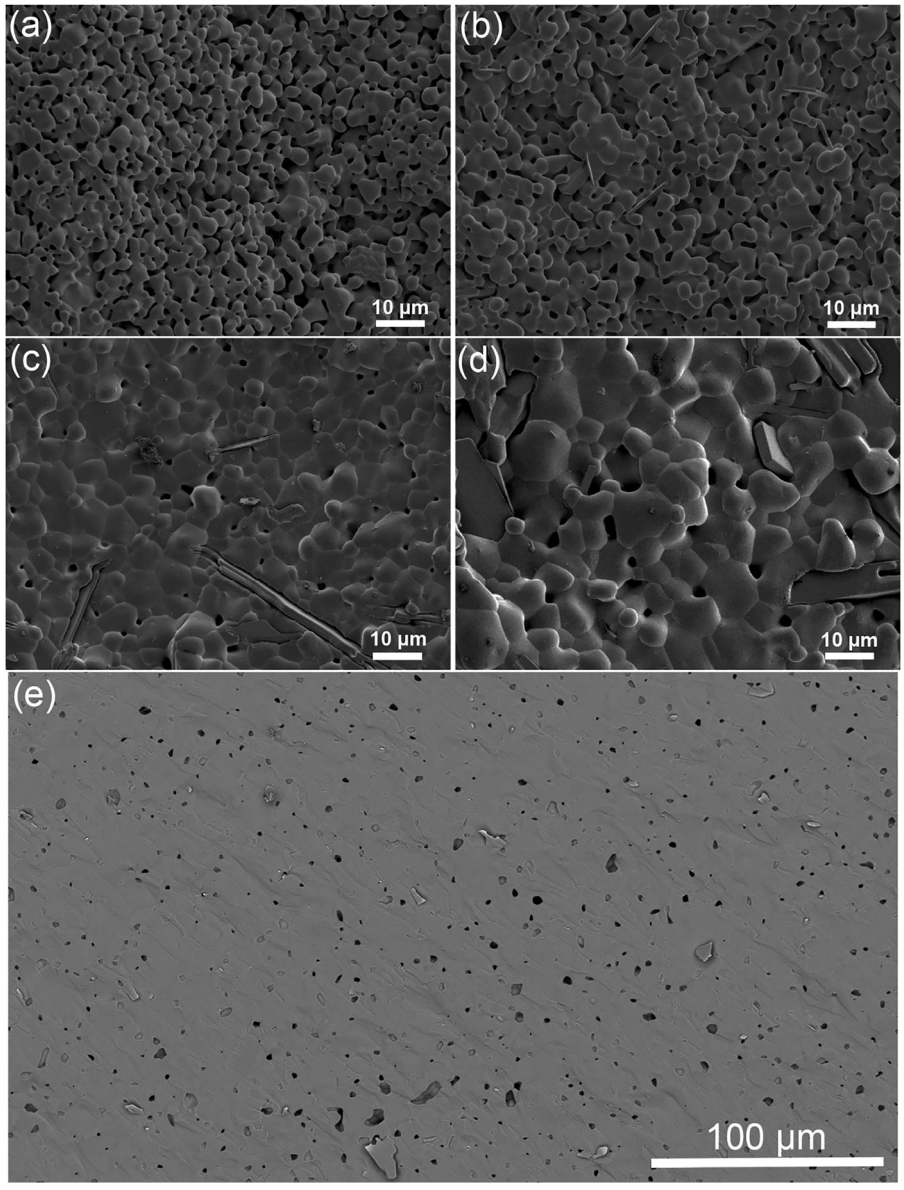

Figure 4. (a–d) SEM images of the surface microstructure of BMO samples sintered at 645°C for 2, 3, 4, and 5 h with 13.59% ±1.41, 11.15% ±0.5, 5.5% ±0.3 and 3.8% ±0.18 porosity, respectively, (e) Cross section SEM image of the sintered sample at 645°C for 4 h.

Ceramics are known as materials with high hardness, brittleness, more resistant to high temperatures and sensitive to thermal shocks. However, previous studies report the SLS of different ceramic materials (Sofia, Barletta, and Poletto 2018; Gahler, Heinrich, and Günster 2006; Bertrand et al. 2007; Tian et al. 2010; Tang, Chiu, and Yen 2011; Basile et al. 2012; Sofia et al. 2015). Thus, SLS can potentially be considered as an alternative to produce multi-material parts through heat treating each material optimally. The greater utilisation of SLS process for ceramics is yet to come.

Table 1. Properties of SLB/sintered BMO (three samples of 24 × 22 × 3 mm sintered at 645°C for 4 h).

Compression Strength (MPa)	Density (g/cm^3)	Total Porosity (%)	Shrinkage (%)		
			Length	Width	Height
4097.4 ± 59.5	6.25 ± 2.0	5.5 ± 0.74	15 ± 0.84	14 ± 0.65	3.22 ± 0.18

Dielectric properties of BMO samples were initially measured between 8–12 GHz in a WR90 waveguide (22.86 × 10.16 mm^2). As shown in Figure 7, ε_r increases from ~10 to 29 after sintering while tan δ decrease from about 0.05 to 0.01. However, to achieve the waveguide dimensions, samples were manually ground and marginally smaller than the cavity, resulting a lower ε_r and parasitic losses from the waveguide/ceramic interface. A TE01δ dielectric resonator method was thus employed which gave $\varepsilon_r = 33.81$ and tan $\delta = 0.0004$, values considerably closer to the bulk ceramic (Zhou et al. 2009). This technique can only measure the dielectric properties at one resonant frequency but is more

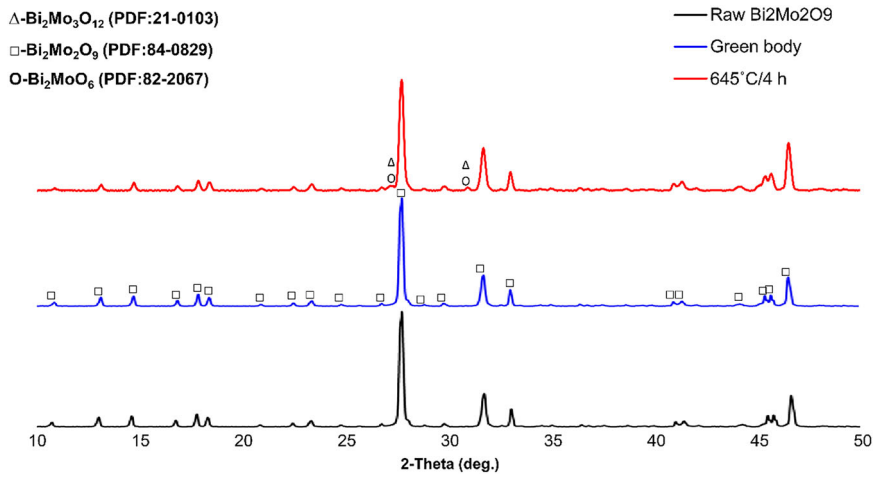

Figure 5. X-Ray diffraction analysis of raw BMO powder, BMO green and sintered bodies.

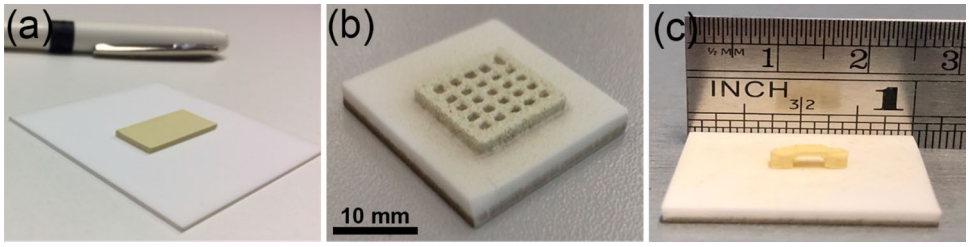

Figure 6. (a,b,c) BMO samples fabricated by the SLB process sintered at 645°C for 4 h.

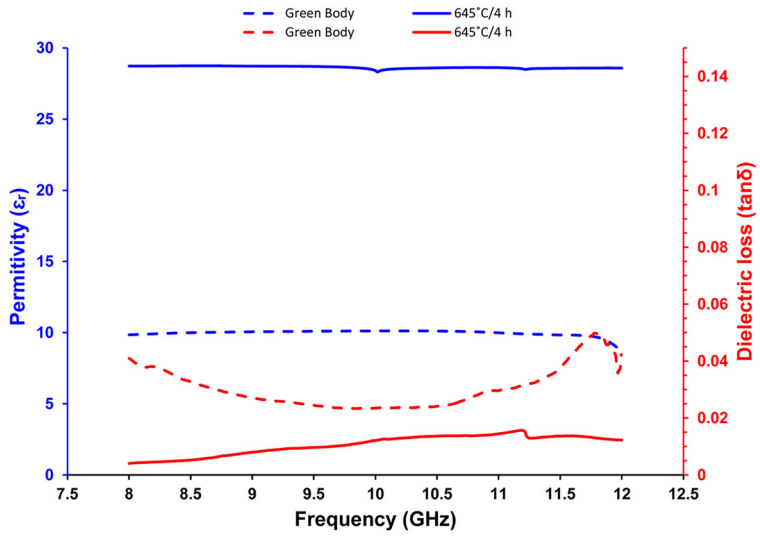

Figure 7. Average dielectric properties of green body and sintered BMO.

likely to represent the true MW properties. Comparison of the results acquired by both measurements techniques at 8 GHz is shown in Table 2.

BMO is reported to have $\varepsilon_r = 38$ (Zhou et al. 2008, 2009; Liu et al. 2010) for phase pure samples with >98% density. The disparity between reported and measured values is attributed to the presence of minor secondary phases and a greater volume faction of porosity, each of which drive ε_r to be lower than BMO bulk ceramics (Zhou et al. 2009). Further studies are underway to improve properties but we note that 3D printed SLB BMO has 3–4 orders of magnitude lower tan δ at 10 GHz than

any known polymer used in AM and an order of magnitude greater ε_r, opening up new design space for miniaturised high frequency RF devices.

Previous research has shown that multi-material structures with Ag floating electrodes in a polymer dielectric host (polyester polylactic acid) are promising for metamaterial applications (Zhang, Whittow, and Vardaxoglou 2017). Ag floating electrodes are used to tailor the effective ε_r and therefore, the feasibility of printing BMO with embedded metallic floating electrodes was investigated. BMO slurry and Ag paste were used to print the host dielectric and metallic electrodes onto Al_2O_3 substrates layer by layer, Figure 8(a,b). BMO layers were scanned by the laser (SLB) after deposition to ensure the structural integrity and promoted bonding between the particles followed by the Ag deposition within the described cavities.

Figure 8(c) shows an optical image of a sintered Ag electrode embedded in the BMO matrix without using SLB which reveals an interaction layer (dark contrast) surrounding the electrode, but by applying the SLB process (Figure 8(d)) this interaction layer is greatly reduced. Figure 8(e) is an SEM image overlaid with an EDS elemental map showing the Ag content (green colour) in the interaction layer. Figure 8(f) is an SEM image of the ceramic surface near the interface between the Ag/BMO in which EDS analysis has identified the regions of $AgBi(MoO_4)_2$ phases which has formed during the reaction of Ag with the BMO. $AgBi(MoO_4)_2$ is known to have a lower sintering temperature than the matrix phase and hence has the appearance of a phase that was molten at the sintering temperature. Cooling to room temperature has resulted in crystallization of the $AgBi(MoO_4)_2$ and the formation of local microcracks.

Although limited through the use of SLB (Figure 9), even the partial reaction of BMO with Ag may well limit this combination of components being used commercially. However, there are a number of low sintering temperature compounds that can be utilised within a slurry that do not react with Ag (Zhou et al. 2017a, 2017b, 2018), thereby eliminating this problem in further iterations in the development of 3D printed RF structures using the SLB.

The BMO dielectric properties are appealing for radio frequency (RF) applications due to its high permittivity, for device miniaturisation, and low loss. A conventional microstrip was designed to demonstrate that the SLB process can form functional devices. For RF circuits 50 Ohms transmission line sections are commonly used to transfer electrical signals around the circuit. The appropriate microstrip line dimensions were calculated using the design equations presented by (Bahl and Garg 1977) assuming a substrate permittivity of 33.81 and a substrate thickness of 3 mm. The calculated characteristic impedance of the transmission line was 48.6 Ohms. A BMO substrate (20 mm × 20 mm × 3 mm) was prepared by the SLB process with a printed Ag transmission line (0.5 mm wide and 0.2 mm high). Copper tape acted as the ground plane, SMA connectors were mounted with super glue and a highly conductive silver ink ($\sigma = 3.33 \times 10^6$) was then used to obtain electrical connection between the SMA outer sheath to the copper tape ground plane and the SMA inner signal pin to the silver transmission line. The SMA connectors allow the transmission line performance to be measured by the vector network analyser.

Figure 10(a) illustrates the microstrip design and Figure 10(b) shows the final device. There were no signs of delamination between the microstrip and substrate. The transmitted power (S_{21}) and the reflected power (S_{11}) measured by the VNA was compared to the results from an electromagnetic simulation in CST Studio (Figure 10(c,d)). The S_{21} parameter displays the proportional power in decibels propagated for one connector to the other whilst the S_{11} parameter displays the proportional power in decibels reflected back to the same connector that launched the signal. As can be seen the curves are in agreement and follow a similar trend. As frequency increases reflections in the line also increase and the transmitted power is reduced. At 4.4 GHz a quarter of the wavelength is approximately equal to the substrate thickness which causes unwanted higher order electromagnetic modes to propagate inside the substrate. The frequency at which other modes start to propagate can be calculated by (Transmission line design 1917):

$$f_c = \frac{c}{4h\sqrt{\varepsilon_r - 1}}$$

Where c is the speed of light in a vacuum (3×10^8), h is the substrate thickness and ε_r is the permittivity of the microstrip transmission line substrate.

By reducing substrate thickness or dielectric constant these higher order modes will be suppressed, and the line will be useable at higher frequencies. As stated, this substrate thickness was chosen to ensure a more reliable print of the silver transmission line, but with a finer nozzle or single line print a thinner line could be printed and the substrate thickness reduced. However, this is a proof of concept that 3D printed BMO and silver structures can be used to create electronic circuits.

Table 2. EM properties of sintered BMO obtained by different measurement techniques at 8 GHz.

Measurement Technique	WR90		TE01δ	
EM Properties	ε_r	tan δ_e	ε_r	tan δ_e
$Bi_2Mo_2O_9$	28.81	0.01	33.81	0.0004

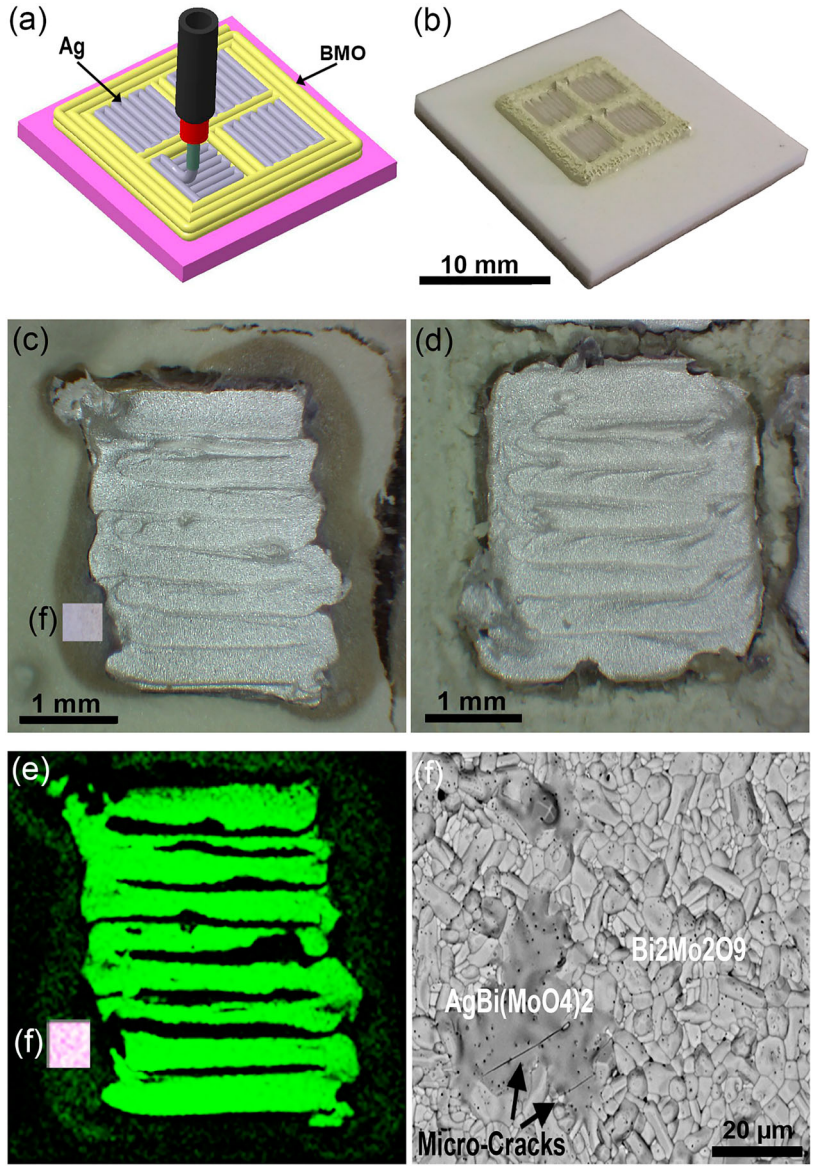

Figure 8. (a,b) Illustration of multi-layers BMO/Ag printing process and a printed green body, respectively, (c,d) micrographs of Ag electrodes embedded in a BMO matrix with reduced and full SLB process, respectively, (e) EDS elemental analysis of Ag content in part (c), green colour represents Ag element, (f) the rectangle labelled in parts (c) and (e) which displays the BMO/Ag interface at higher magnification.

The BMO transmission line achieves a miniaturisation factor of 4.3 compared to propagation in free space as the high permittivity BMO greatly compresses the electromagnetic waves. An example application would be for compact delay lines or miniaturised microstrip antennas due to high wave compression. Reducing the substrate thickness would increase the useable frequency range of the structure whilst adding BMO on top, making an embedded structure, would further increase miniaturisation benefits. Figure 10(e) shows a different example of 3D printed BMO/Ag i.e. capacitively coupled ring resonator such that Ag was printed onto BMO. As this material can be 3D printed unconventional ceramic resonators can also be produced that cannot be made with conventional means.

4. Conclusions

In summary, a 3D printable material system based on co-fired Ag and BMO slurries was developed and processed using SLB to create dense metal-ceramic parts. The SLB process was optimised to achieve near full binder burn-out of the BMO slurries which improved edge definition. Using laser to burn out the binder serves several purposes: (1) The storage modulus of the slurry is high enough to retain the shape of single layers

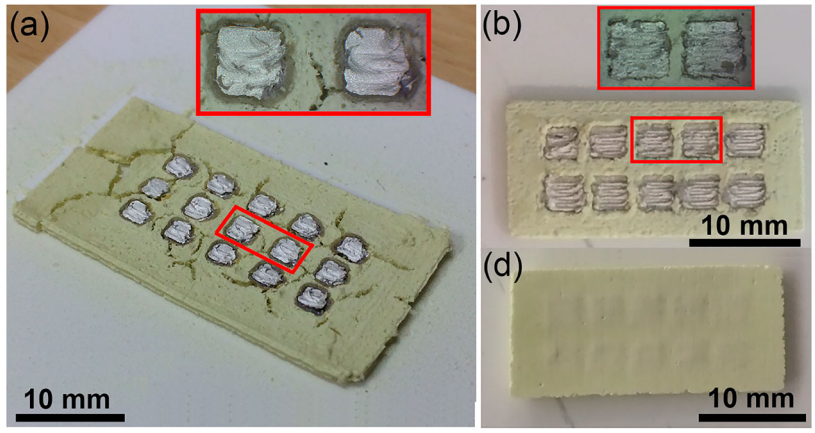

Figure 9. Effect of the SLB process on cracking and interfacial reaction between BMO matrix and embedded Ag electrodes with (a) reduced and, (b,c) full (top and bottom view) SLB process.

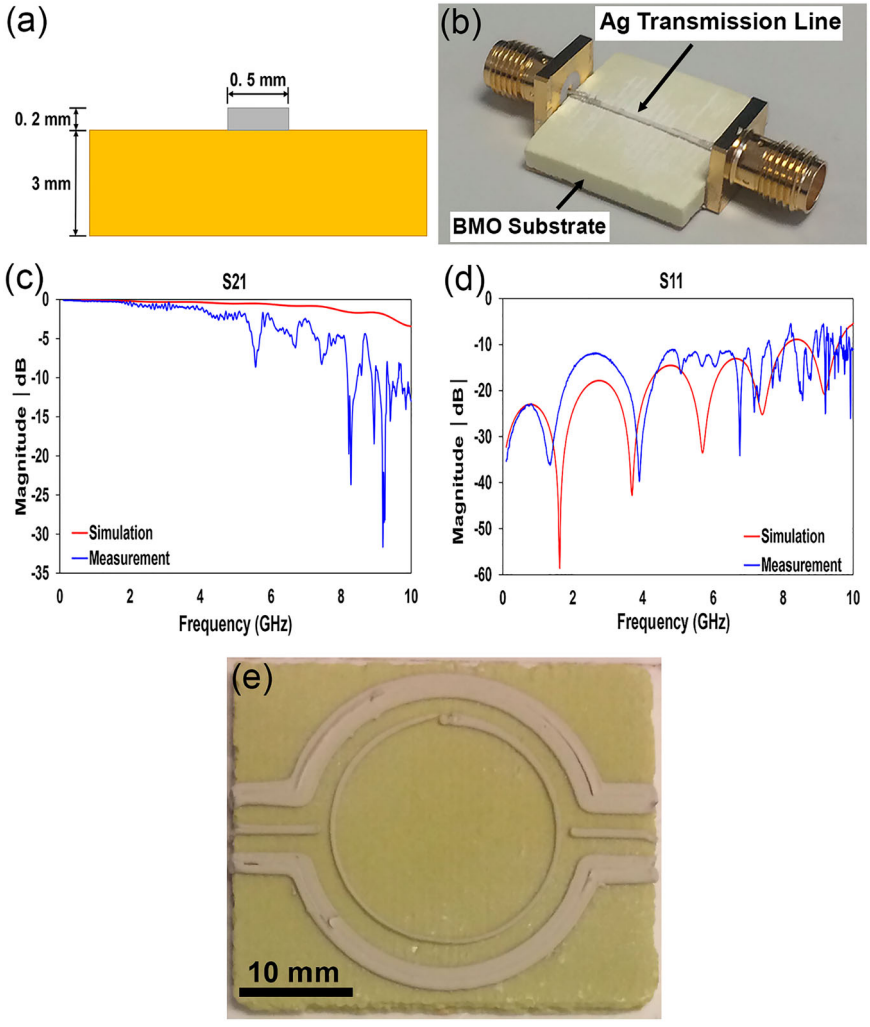

Figure 10. (a) Side view (schematic) of the microstrip made from BMO (yellow) and Ag (grey), (b) fabricated device (20 mm × 20 mm × 3 mm), (c,d) S21 and S11 simulations and measurements results for the fabricated device, respectively, (e) slightly more complex Ag design i.e. a ring resonator printed onto BMO.

(only flows slightly as explained above) but not subsequent layers due to the added weight. Removing the binder layer by layer enables 3D shapes to be made. (2) Removes binder from the Ag paste, thereby greatly reducing the interaction between ceramic and Ag. (3) The shrinkage during sintering is greatly reduced,

which will benefit later complex designs by reducing cracking. (4) Selective partial removal of the binder can tailor the sintering shrinkage so each material in a multi-material samples will shrink equally.

Sintering BMO for 4 h at 645°C resulted in parts with ~95% theoretical density whilst maintain phase assemblage and good mechanical (compressive strength of 4097 MPa) and dielectric ($\varepsilon_r = 33.8$ and tan $\delta = 0.0004$) properties. SLB samples showed little or no Ag leaching but a partial reaction was observed between Ag and BMO upon sintering (Zhou et al. 2009). A conventional microstrip was fabricated and the results showed that the SLB process can form functional devices. The printing resolution used for this investigation was approximately 500 µm resulting in resonance around 4 GHz for a microstrip transmission line ($\varepsilon_r = 33.8$), sufficient for many applications. Further optimisation of the process should enable 100 µm resolution and the substrate dielectric constant can be lowered by design or use of different dielectric material, leading to frequency applications up to approximately 60 GHz. For metamaterials the substrate thickness does not have to be as dominant and the frequency limit could be 100 GHz.

Thus, this study presents the first step towards full 3D design freedom for co-fired, printed ceramic/metal architectures for the communications and electronics communities. It is envisaged that the use of SLB alongside ultra-low temperature sintering dielectrics will enable the direct fabrication of antennas, artificial dielectrics with variable ε_r and 3D metamaterial components for RF and microwave communication with fully integrated feedlines.

Acknowledgements

The authors would also like to thank Dr. Keith Yendall, Mr. Shaun Fowler, and Ms. Dawn Spencer for the kind help with the characterizations and acknowledge use of facilities within the Loughborough Materials Characterisation Centre (LMCC).

Disclosure statement

No potential conflict of interest was reported by the authors.

Funding

This work is supported by the UK's Engineering and Physical Science Research Council through the grant "Synthesizing 3D metamaterials for RF, microwave and terahertz applications", SYMETA, grant reference EP/N010493/1.

Notes on contributors

Reza Gheisari is a Ph.D. researcher at Wolfson school of mechanical, electrical and manufacturing engineering, Loughborough University. His research activities are mainly focused on laser additive manufacturing of ceramics and metals.

Henry Chamberlain pursued an undergraduate degree in mechanical engineering. The focus of his undergraduate project was on 3D printing of high-performance sensors.

Dr George Chi-Tangyie is currently working as a post-doctoral research associate at the Materials Department of Loughborough University.

Dr Shiyu Zhang completed his Ph.D. at Loughborough University in 2014. Following graduation, he has worked as Research Associate in the School. Then he received the EPSRC Doctoral Prize Research Fellowship Award in 2015, carried out research on additive manufacturing novel 3D antennas and metamaterials. He is currently the Project Engineer of the EPSRC multidisciplinary Grand Challenge: Synthesizing 3D Metamaterials for RF, Microwave and THz Applications. His research interests are in additive manufacturing antennas & RF circuit components, metamaterials, heterogenous artificial dielectrics, antennas for millimetre and submillimetre waves application, and wearable antennas & electronic systems.

Dr Athanasios (also known as Thanos) Goulas holds a BEng in Mechanical Engineering from the University of West Attica in Greece, an M.Sc. in Advanced Manufacturing Engineering and Management and a Ph.D. in Mechanical & Manufacturing Engineering from Loughborough University in the United Kingdom. His Ph.D. research focused in additive manufacturing using space resources and in-situ resource utilisation. His current post-doctoral research is focused in electroceramics and development of novel additive manufacturing techniques for realising metamaterial structures for high-frequency RF electronics.

Chih-Kuo (Chuck) Lee is pursuing his Ph.D. degree at Wolfson School of Mechanical, Electrical and Manufacturing Engineering, Loughborough University. His research is mainly focused on dielectric properties measurements.

Tom Whittaker received the M.Eng. degree (first class) in electronic and electrical engineering from Loughborough University, Loughborough, U.K., in 2016. He is currently pursuing the Ph.D. degree. He joined the SYMETA Research Centre (www.symeta.co.uk), Sint-Pieters-Leeuw, Belgium in 2016. His current research interests include equivalent circuit modeling of metamaterials and the design and manufacture of 3D printed metamaterial components for RF and microwave applications.

Dr Dawei Wang is a Research Associate in the Department of Materials Science and Engineering at the University of Sheffield (UK) since 2014. He received his Ph.D. degree from Beijing Institute of Technology (China) in 2012. He was also a Joint Ph.D. student (2010–2011) and a visiting scholar (2016.4-6) at the Materials Research Institute of Pennsylvania State University (USA). His research focuses on the synthesis and characterisation of innovative energy storage/conversion/harvesting materials, and translation of new materials to prototype devices/components for electronic systems. He has published 90+ refereed papers, with a total citation of 1900+ and an H-index of 28 (google scholar). Also, he holds 5 issued patents and has given 10+ invited talks on international conference.

Dr Annapoorani Ketharam received her Ph.D. in 2005 and currently working as a post-doctoral research associate at the Materials Department of Loughborough University. Her

expertise includes development of ceramic material formulations for 2D/3D printing, microwave sintering, conventional sintering, hybrid processing, slip casting and gel casting.

Avishek Ghosh is currently pursuing his Ph.D. at the Materials Department of Loughborough University.

Prof. Bala Vaidhyanathan is the Associate Dean for Enterprise, Professor of Advanced Materials and Processing at the Materials Department of Loughborough University and leads the Advanced Ceramics Group. He has >160 peer-reviewed publications (>3750 citations, H index =33), 7 book chapters and 17 patents. BV has pioneered the development of energy-efficient microwave, hybrid and flash methods for the advanced processing of functional materials and devices including additive manufacturing of ceramics.

Dr Will Whittow (M'12-SM'12) received the B.Sc. degree in physics and the Ph.D. degree in computational electromagnetics from the University of Sheffield, Sheffield, U.K., in 2000 and 2004, respectively. From 2004 to 2012, he was a Research Associate with Loughborough University, Loughborough, U.K. In 2012, he became a Lecturer of electronic materials integration with the University of Loughborough. He became a Senior Lecturer in 2014 and a Reader (Associate Professor) of radio frequency materials in 2018 with the Wolfson School of Mechanical, Electrical and Manufacturing Engineering, Loughborough University. He has authored more than 215 peer-reviewed journal and conference articles in topics related to electromagnetic materials, synthetic dielectrics, dielectric measurements, 3D-printing, wearable antennas, VHF antennas, specific absorption rate, FDTD, specific absorption rate, metamaterials, heterogeneous substrates, embroidered antennas, inkjet printing, electromagnetic compatibility, RFID tags, phantoms and genetic algorithms. His academic journal articles can be freely downloaded via: <http://publications.lboro.ac.U.K./publications/all/collated/elwgw.html>. Dr Whittow was the Coordinating Chair of the Loughborough Antennas and Propagation Conference (LAPC) from 2007 to 2011. In 2017, he was the recipient of the Women in Engineering Men As Allies Award. He is an Associate Editor of Electronics Letters. He serves on the Technical Program Committees for several IEEE international conferences. He has been asked to give 13 invited conference presentations; a 4-day invited workshop on bioelectromagnetics and teach about dielectric measurements at the European School of Antennas.

Dr Darren Cadman received the Ph.D. degree from the Institute of Microwaves and Photonics, University of Leeds, Leeds, U.K., in 2003, that investigated the optical control of microstrip electromagnetic bandgap structures. In 2007, he was with Filtronic Compound Semiconductors Ltd., where he took up the post of managing the Innovative Electronics Manufacturing Research Center based at Loughborough University, Loughborough, U.K. In 2016, he took up the post of Program Manager for the U.K.'s EPSRC funded project Synthesizing 3-D Metamaterials for RF, microwave and terahertz applications led by Loughborough University. His current research interests include the application of additive manufacturing processes to create microwave passive componentry.

Prof. Yiannis C. Vardaxoglou (F'12) received the B.Sc. degree in mathematical physics and the Ph.D. degree in electronics from the University of Kent, Kent, U.K., in 1982 and 1985, respectively. He joined Loughborough University, Loughborough, U.K., as a Lecturer in 1988 and was promoted to Senior Lecturer in 1992 and Professor of wireless communications in 1998. He served as the Dean of the School of Electronic, Electrical, and Systems Engineering with Loughborough University from 2011 to 2012. He established the 30-year-old Wireless Communications Research (WiCR) Group, Loughborough University, and founded the Centre for Mobile Communications Research (CMCR). He is the Director of the SYMETA Research Centre (www.symeta.co.uk), Sint-Pieters-Leeuw, Belgium, funded by an EPSRC Grand Challenge award, researching in wide-ranging topics applicable to cutting-edge wireless communications technology. He has authored over 400 refereed journals and conference proceeding articles (with over 7500 citations) and has written a book on FSS. He holds six patents. His current research focuses primarily on metamaterial structures, additive manufacturing (3D printing) for RF/micro-/millimeter-wave engineering. Dr Vardaxoglou was elected a Fellow of the Royal Academy of Engineers in 2011 and the Institute of Electrical and Electronics Engineers in 2012. He was recently awarded a prestigious EPSRC's Grand Challenge £5M (FEC) Award: Synthesizing 3D Metamaterials for RF, Microwave and THz Applications, (<http://gow.epsrc.ac.uk/NGBOViewGrant.aspx?GrantRef=EP/> N010493/1). He has served as a Consultant to various industries and is the Technical Director of Antrum Ltd. He has attracted research funding from industry and has been awarded 18 EPSRC research grants. He was the Chairman of the Executive Committee of IET's Antennas and Propagation Professional Network in the U.K. and the Chair of the IEEE's distinguish lecturer program of the Antennas and Propagation Society (APS) for five years. He founded the Loughborough Antennas and Propagation Conference (LAPC), which has been running since 2005. He has chaired numerous IEE//IET events and has served on the Steering Committee of the European Conference on Antennas and Propagation, EuCAP. He was the General Chair of EuCAP '07.

Prof. Ian M. Reaney joined the Department of Materials Science and Engineering, University of Sheffield in 1994, as a PDRA, then as a Lecturer from 1995 followed by promotion to a personal chair in 2007, followed by becoming the Dyson Chair in Ceramics in 2016. He attained his Ph.D. from the University of Manchester in 1989 and worked as post-doctoral researcher at the University of Essex before joining the group of Professor Setter at the Laboratoire de Ceramique, Ecole Polytechnique Federale de Lausanne in Switzerland in 1991. He is the European site director for the NSF funded Centre for Dielectrics and Piezoelectrics and the Director of Research and Innovation in MSE.

Dr Daniel Southcott Engstrom received his Ph.D. in 2010 from Technical University of Denmark (DTU). From 2010 to 2015 Daniel was a post doc at Imperial College London, University College London and University of Oxford carrying out research on a variety of projects ranging from nanofluidic filters for HIV detection to additive manufacturing at the nanoscale. He has been a Lecturer in 3D printing at Loughborough University since 2015.

ORCID

Reza Gheisari http://orcid.org/0000-0001-7821-3995

References

Bahl, I. J., and Ramesh Garg. 1977. "Simple and Accurate Formulas for a Microstrip with Finite Strip Thickness." *Proceedings of the IEEE* 65 (11): 1611–1612. doi:10.1109/PROC.1977.10783.

Balla, Vamsi Krishna, Susmita Bose, and Amit Bandyopadhyay. 2010. "Microstructure and Wear Properties of Laser Deposited WC-12%Co Composites." *Materials Science and Engineering A* 527 (24–25): 6677–6682. doi:10.1016/j.msea.2010.07.006.

Basile, Natanaël, Maurice Gonon, Fabrice Petit, and Francis Cambier. 2012. "Interaction Between Laser Beam and BaTiO 3 Powders in Selective Laser Sintering Treatments." *Journal of the European Ceramic Society* 32 (12): 3303–3311. doi:10.1016/j.jeurceramsoc.2012.04.033.

Bertrand, Ph, F. Bayle, C. Combe, P. Goeuriot, and I. Smurov. 2007. "Ceramic Components Manufacturing by Selective Laser Sintering." *Applied Surface Science* 254 (4): 989–992. doi:10.1016/j.apsusc.2007.08.085.

Cai, Kunpeng, Benito Román-Manso, Jim E. Smay, Ji Zhou, María Isabel Osendi, Manuel Belmonte, and Pilar Miranzo. 2012. "Geometrically Complex Silicon Carbide Structures Fabricated by Robocasting." *In Journal of the American Ceramic Society* 95: 2660–2666. doi:10.1111/j.1551-2916.2012.05276.x.

Chartier, T., C. Chaput, F. Doreau, and M. Loiseau. 2002. "Stereolithography of Structural Complex Ceramic Parts." *Journal of Materials Science* 37 (15): 3141–3147. doi:10.1023/A:1016102210277.

Cho, Seo-Yong, Hyuk-Joon Youn, Dong-Wan Kim, Tae-Gyun Kim, and Kug Sun Hong. 2005. "Interaction of BiNbO4-Based Low-Firing Ceramics with Silver Electrodes." *Journal of the American Ceramic Society* 81 (11): 3038–3040. doi:10.1111/j.1151-2916.1998.tb02737.x.

Das, Mitun, Vamsi Krishna Balla, Debabrata Basu, Susmita Bose, and Amit Bandyopadhyay. 2010. "Laser Processing of SiC-Particle-Reinforced Coating on Titanium." *Scripta Materialia* 63 (4): 438–441. doi:10.1016/j.scriptamat.2010.04.044.

Das, Mitun, Sandip Bysakh, Debabrata Basu, T. S. Sampath Kumar, Vamsi Krishna Balla, Susmita Bose, and Amit Bandyopadhyay. 2011. "Microstructure, Mechanical and Wear Properties of Laser Processed SiC Particle Reinforced Coatings on Titanium." *Surface and Coatings Technology* 205 (19): 4366–4373. doi:10.1016/j.surfcoat.2011.03.027.

Faouri, Sinan S., Ali Mostaed, Julian S. Dean, Dawei Wang, Derek C. Sinclair, Shiyu Zhang, William G. Whittow, Yiannis Vardaxoglou, and Ian M. Reaney. 2019. "High Quality Factor Cold Sintered Li 2 MoO 4 –BaFe 12 O 19 Composites for Microwave Applications." *Acta Materialia* 166: 202–207. doi:10.1016/j.actamat.2018.12.057.

Feilden, E. 2017. "Additive Manufacturing of Ceramics and Ceramic Composites via Robocasting." Dissertation. Department of Materials, Imperial College London.

Gahler, André, Jürgen G. Heinrich, and Jens Günster. 2006. "Direct Laser Sintering of Al2O3-SiO2 Dental Ceramic Components by Layer-Wise Slurry Deposition." *Journal of the American Ceramic Society* 89 (10): 3076–3080. doi:10.1111/j.1551-2916.2006.01217.x.

Griffith, Michelle L., and John W. Halloran. 2005. "Freeform Fabrication of Ceramics via Stereolithography." *Journal of the American Ceramic Society* 79 (10): 2601–2608. doi:10.1111/j.1151-2916.1996.tb09022.x.

Gualtieri, Thomas, and Amit Bandyopadhyay. 2018. "Additive Manufacturing of Compositionally Gradient Metal-Ceramic Structures: Stainless Steel to Vanadium Carbide." *Materials and Design* 139: 419–428. doi:10.1016/j.matdes.2017.11.007.

Hinczewski, C., S. Corbel, and T. Chartier. 1998. "Ceramic Suspensions Suitable for Stereolithography." *Journal of the European Ceramic Society* 18 (6): 583–590. doi:10.1016/s0955-2219(97)00186-6.

Jafari, M. A., W. Han, F. Mohammadi, A. Safari, S. C. Danforth, and N. Langrana. 2000. "A Novel System for Fused Deposition of Advanced Multiple Ceramics." *Rapid Prototyping Journal* 6 (3): 161–174. doi:10.1108/13552540010337047.

Jakus, Adam E., Shannon L. Taylor, Nicholas R. Geisendorfer, David C. Dunand, and Ramille N. Shah. 2015. "Metallic Architectures from 3D-Printed Powder-Based Liquid Inks." *Advanced Functional Materials* 25 (45): 6985–6995. doi:10.1002/adfm.201503921.

Lewis, Jennifer A., James E. Smay, John Stuecker, and Joseph Cesarano. 2006. "Direct Ink Writing of Three-Dimensional Ceramic Structures." *Journal of the American Ceramic Society* 89 (12): 3599–3609. doi:10.1111/j.1551-2916.2006.01382.x.

Liu, Z. H., J. J. Nolte, J. I. Packard, G. Hilmas, F. Dogan, and M. C. Leu. 2007. "Selective Laser Sintering of High-Density Alumina Ceramic Parts." In *Proceedings of the 35th International MATADOR 2007 Conference*, 351–354. doi:10.1007/978-1-84628-988-0_79.

Liu, Weihong, Hong Wang, Di Zhou, and Kecheng Li. 2010. "Dielectric Properties of Low-Firing Bi 2 Mo 2 O 9 Thick Films Screen Printed on Al Foils and Alumina Substrates." *Journal of the American Ceramic Society* 93 (8): 2202–2206. doi:10.1111/j.1551-2916.2010.03719.x.

Lu, Xuesong, Yoonjae Lee, Shoufeng Yang, Yang Hao, Julian R G Evans, and Clive G. Parini. 2009. "Fine Lattice Structures Fabricated by Extrusion Freeforming: Process Variables." *Journal of Materials Processing Technology* 209 (10): 4654–4661. doi:10.1016/j.jmatprotec.2008.11.039.

Maazouz, Y., E. B. Montufar, J. Guillem-Marti, I. Fleps, C. Öhman, C. Persson, and M. P. Ginebra. 2014. "Robocasting of Biomimetic Hydroxyapatite Scaffolds Using Self-Setting Inks." *Journal of Materials Chemistry B* 2 (33): 5378–5386. doi:10.1039/c4tb00438h.

Man, H. C., S. Zhang, F. T. Cheng, and T. M. Yue. 2001. "Microstructure and Formation Mechanism of in Situ Synthesized TiC/Ti Surface MMC on Ti-6Al-4V by Laser Cladding." *Scripta Materialia* 44 (12): 2801–2807. doi:10.1016/S1359-6462(01)00977-0.

Nurminen, Janne, Jonne Näkki, and Petri Vuoristo. 2009. "Microstructure and Properties of Hard and Wear Resistant MMC Coatings Deposited by Laser Cladding." *International Journal of Refractory Metals and Hard Materials* 27 (2): 472–478. doi:10.1016/j.ijrmhm.2008.10.008.

Pang, W., H. C. Man, and T. M. Yue. 2005. "Laser Surface Coating of Mo–WC Metal Matrix Composite on Ti6Al4 V Alloy." *Materials Science and Engineering* 2005: 144–153.

Parke, L., I. R. Hooper, E. Edwards, N. Cole, I. J. Youngs, A. P. Hibbins, and J. R. Sambles. 2015. "Independently Controlling Permittivity and Diamagnetism in Broadband, Low-Loss, Isotropic Metamaterials at Microwave Frequencies." *Applied Physics Letters* 106: 10. doi:10.1063/1.4915097.

Peng, Erwin, Xiangxia Wei, Ulf Garbe, Dehong Yu, Brunet Edouard, Aihong Liu, and Jun Ding. 2018. "Robocasting of Dense Yttria-Stabilized Zirconia Structures." *Journal of Materials Science* 53 (1): 247–273. doi:10.1007/s10853-017-1491-x.

Reaney, Ian M., and David Iddles. 2006. "Microwave Dielectric Ceramics for Resonators and Filters in Mobile Phone Networks." *Journal of the American Ceramic Society* 89 (7): 2063–2072. doi:10.1111/j.1551-2916.2006.01025.X.

Sahasrabudhe, Himanshu, and Amit Bandyopadhyay. 2016. "Additive Manufacturing of Reactive In Situ Zr Based Ultra-

High Temperature Ceramic Composites." *JOM: Journal of the Minerals Metals and Materials Society* 68 (3): 822–830. doi:10.1007/s11837-015-1777-x.

Sebastian, Mailadil Thomas, Hong Wang, and Heli Jantunen. 2016. "Low Temperature Co-Fired Ceramics with Ultra-Low Sintering Temperature: A Review." *Current Opinion in Solid State and Materials Science*, doi:10.1016/j.cossms.2016.02.004.

Sofia, Daniele, Diego Barletta, and Massimo Poletto. 2018. "Laser Sintering Process of Ceramic Powders: The Effect of Particle Size on the Mechanical Properties of Sintered Layers." *Additive Manufacturing* 23: 215–224. doi:10.1016/j.addma.2018.08.012.

Sofia, Daniele, Mirko Granese, Diego Barletta, and Massimo Poletto. 2015. "Laser Sintering of Unimodal Distributed Glass Powders of Different Size." *Procedia Engineering* 102: 749–758. doi:10.1016/j.proeng.2015.01.180.

Tang, Hwa Hsing, Ming Lu Chiu, and Hsiao Chuan Yen. 2011. "Slurry-Based Selective Laser Sintering of Polymer-Coated Ceramic Powders to Fabricate High Strength Alumina Parts." *Journal of the European Ceramic Society* 31 (8): 1383–1388. doi:10.1016/j.jeurceramsoc.2011.02.020.

Tang, Hwa Hsing, and Hsiao Chuan Yen. 2015. "Slurry-Based Additive Manufacturing of Ceramic Parts by Selective Laser Burn-Out." *Journal of the European Ceramic Society* 35 (3): 981–987. doi:10.1016/j.jeurceramsoc.2014.10.019.

Tian, Xiaoyong, Jens Günster, Jörg Melcher, Dichen Li, and Jürgen G. Heinrich. 2009. "Process Parameters Analysis of Direct Laser Sintering and Post Treatment of Porcelain Components Using Taguchi's Method." *Journal of the European Ceramic Society* 29 (10): 1903–1915. doi:10.1016/j.jeurceramsoc.2008.12.002.

Tian, Xiaoyong, Bo Sun, Jürgen G. Heinrich, and Dichen Li. 2010. "Stress Relief Mechanism in Layer-Wise Laser Directly Sintered Porcelain Ceramics." *Materials Science and Engineering A* 527 (7–8): 1695–1703. doi:10.1016/j.msea.2009.10.058.

Transmission line design. 1917. Trans. Am. Inst. Electr. Eng. 36: 735–788.

Tuttle, Bruce A., James E. Smay, Joseph Cesarano, James A. Voigt, Timothy W. Scofield, Walter R. Olson, and Jennifer A. Lewis. 2001. "Robocast Pb(Zr 0.95 Ti 0.05)O 3 Ceramic Monoliths and Composites." *Journal of the American Ceramic Society* 84 (4): 872–874. doi:10.1111/j.1151-2916.2001.tb00756.x.

Walia, Sumeet, Charan M. Shah, Philipp Gutruf, Hussein Nili, Dibakar Roy Chowdhury, Withawat Withayachumnankul, Madhu Bhaskaran, and Sharath Sriram. 2015. "Flexible Metasurfaces and Metamaterials: A Review of Materials and Fabrication Processes at Micro- and Nano-Scales." *Applied Physics Reviews*, doi:10.1063/1.4913751.

Wang, Dawei, Di Zhou, Shiyu Zhang, Yiannis Vardaxoglou, Willian G. Whittow, Darren Cadman, and Ian M. Reaney. 2018. "Cold-Sintered Temperature Stable Na 0.5 Bi 0.5 MoO 4 -Li 2 MoO 4 Microwave Composite Ceramics." *ACS Sustainable Chemistry and Engineering* 6 (2): 2438–2444. doi:10.1021/acssuschemeng.7b03889.

Yen, Hsiao Chuan. 2012. "A New Slurry-Based Shaping Process for Fabricating Ceramic Green Part by Selective Laser Scanning the Gelled Layer." *Journal of the European Ceramic Society* 32 (12): 3123–3128. doi:10.1016/j.jeurceramsoc.2012.04.014.

Zhang, Yanning, and Amit Bandyopadhyay. 2018. "Direct Fabrication of Compositionally Graded Ti-Al 2 O 3 Multi-Material Structures Using Laser Engineered Net Shaping." *Additive Manufacturing* 21: 104–111. doi:10.1016/j.addma.2018.03.001.

Zhang, Yanning, Himanshu Sahasrabudhe, and Amit Bandyopadhyay. 2015. "Additive Manufacturing of Ti-Si-N Ceramic Coatings on Titanium." *Applied Surface Science* 346: 428–437. doi:10.1016/j.apsusc.2015.03.184.

Zhang, Shiyu, William Whittow, and John (Yiannis) C. Vardaxoglou. 2017. "Additively Manufactured Artificial Materials with Metallic Meta-Atoms." *IET Microwaves, Antennas and Propagation* 11 (14): 1955–1961. doi:10.1049/iet-map.2016.0952.

Zhao, Santuan, Wei Xiao, Mohamed N. Rahaman, David O'Brien, Jacob W. Seitz-Sampson, and B. Sonny Bal. 2017. "Robocasting of Silicon Nitride with Controllable Shape and Architecture for Biomedical Applications." *International Journal of Applied Ceramic Technology* 14 (2): 117–127. doi:10.1111/ijac.12633.

Zheng, B. J., X. M. Chen, and J. S. Lian. 2010. "Microstructure and Wear Property of Laser Cladding Al + SiC Powders on AZ91D Magnesium Alloy." *Optics and Lasers in Engineering* 48 (5): 526–532. doi:10.1016/j.optlaseng.2010.01.001.

Zhong, Lisheng, Fangxia Ye, Yunhua Xu, and Jinshan Li. 2014. "Microstructure and Abrasive Wear Characteristics of in Situ Vanadium Carbide Particulate-Reinforced Iron Matrix Composites." *Materials and Design* 54: 564–569. doi:10.1016/j.matdes.2013.08.097.

Zhou, Di, Jing Li, Li Xia Pang, Da Wei Wang, and Ian M. Reaney. 2017a. "Novel Water Insoluble (Na x Ag 2-x) MoO 4 ($0 \leq x \leq 2$) Microwave Dielectric Ceramics with Spinel Structure Sintered at 410 Degrees." *Journal of Materials Chemistry C* 5 (24): 6086–6091. doi:10.1039/c7tc01718a.

Zhou, Di, Li Xia Pang, Da Wei Wang, Chun Li, Biao Bing Jin, and Ian M. Reaney. 2017b. "High Permittivity and Low Loss Microwave Dielectrics Suitable for 5G Resonators and Low Temperature Co-Fired Ceramic Architecture." *Journal of Materials Chemistry C* 5 (38): 10094–10098. doi:10.1039/c7tc03623j.

Zhou, Di, Li Xia Pang, Da Wei Wang, Ze Ming Qi, and Ian M. Reaney. 2018. "High Quality Factor, Ultralow Sintering Temperature Li 6 B 4 O 9 Microwave Dielectric Ceramics with Ultralow Density for Antenna Substrates." *ACS Sustainable Chemistry and Engineering* 6 (8): 11138–11143. doi:10.1021/acssuschemeng.8b02755.

Zhou, Di, Li Xia Pang, Da Wei Wang, and Ian M. Reaney. 2019. "Novel Water-Assisting Low Firing MoO 3 Microwave Dielectric Ceramics." *Journal of the European Ceramic Society* 39 (7): 2374–2378. doi:10.1016/j.jeurceramsoc.2019.01.052.

Zhou, Di, Clive A. Randall, Amanda Baker, Hong Wang, Li Xia Pang, and Xi Yao. 2010. "Dielectric Properties of an Ultra-Low-Temperature Cofiring Bi 2 Mo 2 O 9 Multilayer." *Journal of the American Ceramic Society* 93 (5): 1443–1446. doi:10.1111/j.1551-2916.2010.03602.x.

Zhou, Di, Hong Wang, Li Xia Pang, Clive A. Randall, and Xi Yao. 2009. "Bi 2 O 3 -MoO 3 Binary System: An Alternative Ultralow Sintering Temperature Microwave Dielectric." *Journal of the American Ceramic Society* 92 (10): 2242–2246. doi:10.1111/j.1551-2916.2009.03185.x.

Zhou, Di, Hong Wang, Xi Yao, and Li Xia Pang. 2008. "Dielectric Behavior and Cofiring with Silver of Monoclinic BiSbO 4 Ceramic." *Journal of the American Ceramic Society* 91 (4): 1380–1383. doi:10.1111/j.1551-2916.2008.02302.x.

Ziolkowski, Richard W. 2003. "Design, Fabrication, and Testing of Double Negative Metamaterials." *IEEE Transactions on Antennas and Propagation* 51 (7): 1516–1529. doi:10.1109/TAP.2003.813622.